Effect of cell shape and packing density on granulosa cell proliferation and formation of multiple layers during early follicle development in the ovary

Patricia Da Silva-Buttkus[1], Gayani S. Jayasooriya[1], Jocelyn M. Mora[1], Margaret Mobberley[2], Timothy A. Ryder[2], Marianne Baithun[1], Jaroslav Stark[3], Stephen Franks[1] and Kate Hardy[1,*]

[1]Institute of Reproductive and Developmental Biology, Imperial College London, Hammersmith Hospital, Du Cane Road, London W12 0NN, UK
[2]Department of Histopathology, Charing Cross Hospital, Fulham Palace Road, London W6 8RF, UK
[3]Department of Mathematics and Centre for Integrative Systems Biology at Imperial College (CISBIC), Imperial College London, London SW7 2AZ, UK
*Author for correspondence (e-mail: k.hardy@imperial.ac.uk)

Accepted 20 August 2008
Journal of Cell Science 121, 3890-3900 Published by The Company of Biologists 2008
doi:10.1242/jcs.036400

Summary

The postnatal mouse ovary is rich in quiescent and early-growing oocytes, each one surrounded by a layer of somatic granulosa cells (GCs) on a basal lamina. As oocytes start to grow the GCs change shape from flattened to cuboidal, increase their proliferation and form multiple layers, providing a unique model for studying the relationship between cell shape, proliferation and multilayering within the context of two different intercommunicating cell types: somatic and germ cells. Proliferation of GCs was quantified using immunohistochemistry for Ki67 and demonstrated that, unusually, cuboidal cells divided more than flat cells. As a second layer of GCs started to appear, cells on the basal lamina reached maximum packing density and the axes of their mitoses became perpendicular to the basal lamina, resulting in cells dividing inwards to form second and subsequent layers. Proliferation of basal GCs was less than that of inner cells. Ultrastructurally, collagen fibrils outside the basal lamina became more numerous as follicles developed. We propose that the basement membrane and/or theca cells that surround the follicle provide an important confinement for rapidly dividing columnar cells so that they attain maximum packing density, which restricts lateral mitosis and promotes inwardly oriented cell divisions and subsequent multilayering.

Supplementary material available online at
http://jcs.biologists.org/cgi/content/full/121/23/3890/DC1

Key words: Basal lamina, Cell division, Cell shape, Granulosa cells, Multilayering, Ovary, Theca cells

Introduction

Immature non-growing oocytes in the mammalian ovary are each surrounded by a single layer of flattened epithelial cells lying on a basal lamina, forming units known as primordial follicles. As the oocyte starts to grow, these epithelial cells change shape and become cuboidal, before forming multiple layers. In mice, primordial follicles are formed during the first few days following birth, and some of these initiate growth immediately. From this time on, a steady trickle of follicles enter the growing phase. The presence of follicles at different stages of early growth in close proximity to each other makes the postnatal ovary a new model for studying cell shape change and the formation of multiple layers (Fig. 1). Much of our current knowledge of the relationship between cell shape and behaviour is derived from studies of monolayer cultures in vitro. By contrast, the postnatal ovary provides a high density of epithelial cells at varying stages of cuboidalisation, which are undergoing their change in shape in vivo – within a local 3D environment that retains 'normal' cell-cell and cell-extracellular matrix (ECM) interactions. Here, we have exploited this model to examine the relationship between cell shape, proliferation, packing density and multilayering in vivo.

The regulation of entry of follicles into the growing phase is poorly understood in all mammals, including mice. This is surprising, considering the almost exclusive use of murine models for studying the role of a wide variety of genes in development, fertility and ovarian function (Matzuk and Lamb, 2002). Furthermore, the transition from quiescence to growth is crucial and must have a role in defining the reproductive lifespan of the female; too few growing follicles could result in anovulatory cycles, whereas too many could result in premature ovarian failure. Increased understanding of the cellular events that occur during initiation of follicle growth will help to determine how they are regulated.

Initiation of follicle growth is associated with oocyte growth, division of the epithelial granulosa cells (GCs) and a dramatic transformation of GC morphology from flattened to cuboidal (Fig. 1A) (Hirshfield, 1991; Picton, 2001). However, these cellular events have not been well characterised, nor is it clear how they are related. In other tissues and cell types, in vitro studies have demonstrated that modulating cell shape affects cell proliferation, and that flattened non-transformed cells divide more than round cells (Chen et al., 1997; Folkman and Moscona, 1978). Paradoxically, in the ovary, descriptive studies suggest that the opposite is true, with cuboidal cells dividing more than flat cells (Gougeon and Busso, 2000; Lundy et al., 1999; Wandji et al., 1997; Wandji et al., 1996), confirmed in a recent quantitative study using human ovary (Stubbs et al., 2007).

As the GCs cuboidalise, a glycoprotein layer – the zona pellucida – forms between the GCs and the oocyte, which maintain extensive

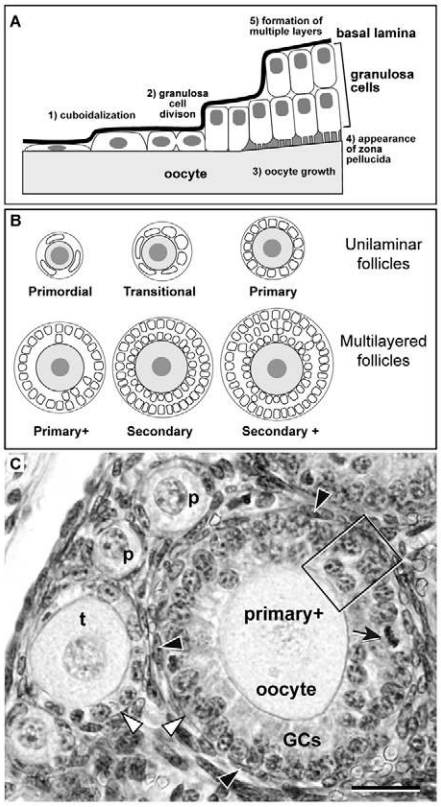

Fig. 1. (A) Summary of cellular changes that take place during initiation of follicle growth. (B) Stages of follicle development analysed in this study. (C) Ovary section stained with H&E, showing examples of follicles at primordial (p), transitional (t) and primary-plus stage. In the primary-plus follicle the majority of GCs are columnar and form a single layer (GCs), although there are some areas that start to show signs of multilayering (e.g. boxed area). Note basement membrane (white arrowheads), theca cells (black arrowheads) and GCs undergoing mitosis (black arrow). Scale bar: 20 μm.

contact with each other via transzonal processes (TZPs); the latter emanate from the GCs and traverse the zona (Albertini et al., 2001). When the oocyte is surrounded by a complete layer of cuboidal GCs, it is termed a primary follicle. GC proliferation continues and multiple layers of GCs form (Fig. 1B,C). At the primary stage, a layer of flattened cells, the theca-cell layer, is recruited from the stromal cells to envelop the basement membrane (Fig. 1C).

A unique microenvironment in the follicle is maintained by the follicular basal lamina which completely encloses the GCs, expanding as the follicle grows and separating the oocyte and surrounding GCs from adjacent theca, stromal and interstitial cells. The basal lamina excludes blood vessels and nerves from the GC-oocyte unit until after ovulation and, unlike the zona pellucida, is not traversed by any cells or cell processes (Rodgers et al., 2003). In a wide variety of tissues, basal laminae provide support and anchorage for polarised epithelial cells and also regulate their behaviour (cell shape, proliferation, apoptosis, differentiation and migration) (Berkholtz et al., 2006b; Monniaux et al., 2006). A direct transmembrane link between the ECM and the actin cytoskeleton is provided by integrins, which are expressed in the ovary and have a significant role in the regulation of cell behaviour in a wide range of tissues (Burns et al., 2002; Monniaux et al., 2006). Furthermore, basal laminae can act both as a sieve, selectively regulating passage of large macromolecules, and as a reservoir, binding certain growth factors (LeBleu et al., 2007; Rodgers et al., 2003).

In this study, using detailed morphometry and immunohistochemistry for the cell-cycle protein Ki67 in mouse ovary, we have carried out a quantitative analysis of GC proliferation during initiation of follicle growth and the development of the second and third layers of GCs. We compared GC proliferation, the growth trajectory of oocytes and change in GC cell shape on day 12 post partum (pp) (in the presence of only preantral follicles) with that on day 21 pp (in the presence of a wider range of follicle stages including preantral and antral follicles). We examined how changes in GC shape and oocyte growth relate to GC proliferation. Finally, we investigated how the packing density of GCs on the basal lamina induces the formation of multiple layers of GCs by regulating the orientation of the axis of mitosis, and examined how the position of GCs relative to the basal lamina regulates proliferation.

Results

Change in GC shape

In primordial follicles the GCs were flattened (Fig. 2A), and close contact with the oocyte was mediated by desmosome-like junctions (Fig. 2B). The GCs were enveloped in a basal lamina. GC nuclei were also flattened. Flat cells in primordial follicles could be very thin (Fig. 2A), with cytoplasmic extensions as slender as 90 nm. As follicles started to grow, GCs became cuboidal (Fig. 2C), and then more columnar and polarised with the nucleus lying close to the basal lamina (Fig. 2D). Immunolabelling for β-catenin, a protein closely associated with cadherins in the cell membrane, showed membrane localisation and clearly demonstrated the polarised columnar nature of GCs in primary follicles that were developing a second layer (Fig. 2E). The formation of the second layer followed a consistent pattern (Fig. 2F). The single layer of cuboidal or columnar cells formed a continuous and even layer with the basal surfaces of the GCs contacting the basal lamina (Fig. 2F,G) via hemidesmosomes (Fig. 2G), and the apical surface contacting the oocyte via desmosome-like junctions on TZPs (Fig. 2H,I). The second layer of GCs always formed as an inner layer, initially with occasional scattered cells (Fig. 2F) which increased in number (Fig. 2J), while the continuity of the densely packed GCs on the basal lamina was maintained. A layer of flattened theca cells outside the basal lamina was observed from the primary stage onwards (Fig. 2F).

Follicle development, oocyte growth and number of GCs

Two sections from a single ovary from each of eight pups (four on day 12 and four on day 21) were immunohistochemically labelled for Ki67. To ensure that the follicle and oocyte were being analysed and measured at the widest point, only follicles containing an oocyte with a clear nuclear membrane, and/or one or more nucleoli, were assessed (682 follicles in total) (Table 1). On both days (day 12 and day 21), the majority of the follicles were at the primordial stage (Table 1). On day 12, the most advanced follicles were developing a third layer of GCs, whereas on day 21 multilayered preantral and small antral follicles were present. As this study was focusing on the earliest stages of follicle growth, only follicles up the secondary plus stage were examined in detail.

There was significant oocyte growth from the primordial stage onwards (Fig. 3A). The mean oocyte diameter in primordial follicles on day 12 was significantly greater than that on day 21. On day 21, oocytes in follicles which were developing multiple

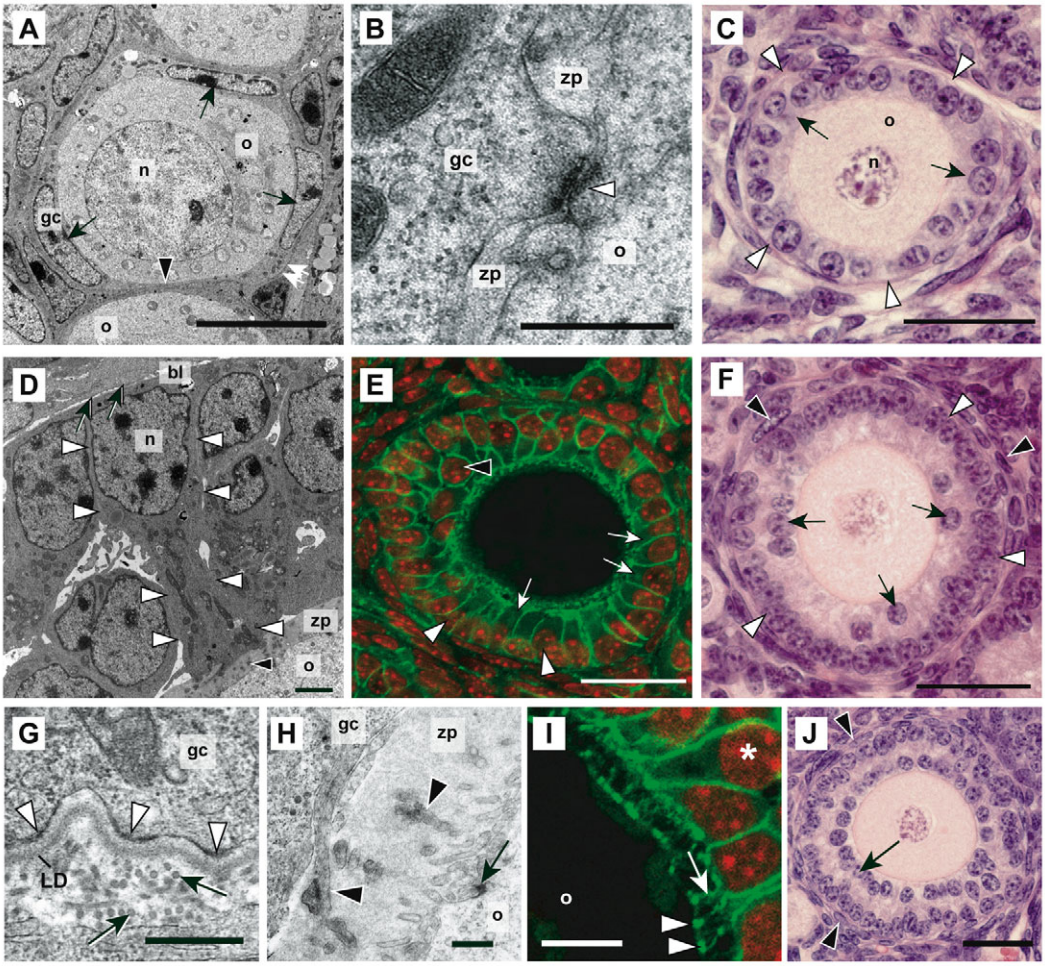

Fig. 2. (A-J) Transmission electron micrographs (A,B,D,G,H), light micrographs (C,F,J) and confocal images (E,I) showing change in GC shape from the primordial to the secondary stages of follicle development. (A) Primordial follicle in day 12 ovary. Three flat GCs are visible in this section, with flattened nuclei (arrows). The GCs are bounded by a basal lamina (double arrow). Note thin GCs between adjacent oocytes (arrowhead); n, oocyte nucleus, o, oocyte cytoplasm, gc, granulosa cell. Scale bar: 10 µm. (B) Desmosome-like junction (arrowhead) between GC and oocyte in day 10 primordial follicle. Note formation of zona pellucida (zp). Scale bar: 500 nm. (C) Primary follicle stained using H&E with a single layer of cuboidal GCs (black arrows). Position of basement membrane marked (white arrowheads). Scale bar: 30 µm. (D) Columnar, polarised GC spanning from basal lamina (bl, arrows) to oocyte (o), with transzonal processes (TZPs) (black arrowhead) traversing zp. GC nucleus (n) abuts basal lamina and GC membrane tracked by white arrowheads. Scale bar: 2 µm. (E) Confocal image of primary-plus follicle immunolabelled for β-catenin (green) with second GC layer developing (black arrowhead) and columnar GCs (arrowed). Note polarised nuclei labelled with DAPI (false-coloured red; white arrowheads) close to basal lamina. Scale bar: 30 µm. (F) Primary plus follicle with a new second layer of GCs (black arrows) developing close to the oocyte. Note the continuity and tight packing of the first layer on the basal lamina (white arrowheads), and developing theca layer (black arrowheads). Scale bar: 30 µm. (G) GC (gc) on basal lamina, with lamina densa (LD) clearly visible, as are hemidesmosomes (white arrowheads) and collagen fibrils (black arrows). Scale bar: 500 nm. (H) TZPs (black arrowheads) from GC (gc) traversing zona pellucida (zp). Note desmosome-like junction (black arrow) at contact with oocyte (o). Scale bar: 500 nm. (I) High-magnification view of columnar GC (asterisk) and TZPs (arrowed) contacting oocyte (o). Note β-catenin staining of TZPs (green), with bright punctate spots where TZPs contact the oocyte (arrowheads). Scale bar: 10 µm. (J) Secondary follicle with two complete layers of GCs (arrowed). Note the developing theca layer (black arrowheads). Scale bar: 30 µm.

layers of GCs were significantly larger than those on day 12 (Fig. 3A). Oocytes and follicles with more than two layers of GCs are likely not to have had sufficient time by day 12 to grow as much as similar follicles on day 21. The number of GCs increased significantly as follicle development progressed (Fig. 3B). During the early stages of follicle development, the number of GCs was remarkably similar on days 12 and 21. However, on day 21 there were significantly more GCs as the third layer of GCs developed, compared to day 12 (Fig. 3B). It is most probable that follicles on day 12 had only just reached the stage of forming a third layer and, therefore, had fewer GCs than similar, well-established follicles on day 21. GC height increased approximately sixfold from the primordial stage to the stage when a few cells were starting to appear in the second layer (Fig. 3C).

Ki67 immunolabelling and follicle stage

The prevalence of Ki67 immunolabelling of GCs was low in the cortex, where the majority of primordial follicles are located, and increased in larger follicles towards the medulla of the ovary (Fig. 4A). Quantitative analysis demonstrated Ki67 labelling in a small proportion of primordial follicles, and a larger proportion of transitional follicles. All follicles from the primary stage onwards contained Ki67-positive GCs (Fig. 4B). The Ki67 labelling index increased significantly as GCs became cuboidal (primordial to

Table 1. Number of follicles at each stage and total number of GCs analysed for Ki67 staining on days 12 and 21 post partum

	Number of follicles		Total number of GCs	
Stage	Day 12	Day 21	Day 12	Day 21
Primordial	360	104	1313	354
Transitional	78	33	633	249
Primary	13	6	293	153
Primary plus	41	15	2269	799
Secondary	9	0	687	–
Secondary plus	7	16	673	1778
Total	508	174	5868	3333

On day 21 no secondary follicles with precisely two layers of GCs were observed.

primary stages). As the follicles acquired further layers of GCs, there was no significant change in the labelling index on either day 12 or day 21 (Fig. 4C). The proportion of primordial and transitional follicles containing Ki67-positive GCs and the labelling index throughout early follicle development was significantly lower on day 21 than on day 12 (Fig. 4B,C).

Another useful marker of proliferation is minichromosome maintenance protein 2 (MCM2), which we have recently used as a marker of GC proliferation in human follicles (Stubbs et al., 2007). MCM2 is present in nuclei throughout the cell cycle but absent in differentiated or quiescent cells (Laskey, 2005). Double immunofluorescence labelling for Ki67 and MCM2 showed that the majority of cells in primordial follicles (Fig. 4D) and some cells in primary follicles (Fig. 4E) were completely unlabelled, suggesting that they were in G0.

Ki67 immunolabelling and cell shape

The proportion of Ki67-positive flat and cuboidal cells was computed overall, for all follicles analysed (Fig. 5A), and for primordial, transitional and primary follicles separately (Fig. 5B). Whereas the majority of flat cells were Ki67-negative (Fig. 5C), a few Ki67-positive flat cells were observed (Fig. 5D); however, a higher proportion of cuboidal cells were Ki67-positive (Fig. 5E,F). Overall, proliferation was around fivefold higher in cuboidal cells compared with flat cells (Fig. 5A). The proportion of Ki67-positive flat cells was similar in primordial and transitional follicles and significantly lower than the proportion of positive cuboidal cells (Fig. 5B), both on day 12 and day 21. In transitional follicles, on day 12 (but not on day 21), the cuboidal cells were immunolabelled more frequently than the flat cells. At the primary stage over a quarter of the cuboidal GCs were Ki67-positive on day 12 (Fig. 5B).

GC shape change, Ki67 immunolabelling and oocyte growth

First we examined whether the change in cell shape or onset of proliferation was associated with oocyte growth. Considering just transitional follicles, containing a mixture of flattened and cuboidal cells, there was no increase in oocyte size with an increasing proportion of cuboidal cells (Fig. 6A), therefore change in GC shape was not associated with oocyte growth. In addition, the onset of proliferation was not associated with oocyte growth. Ki67-positive primordial follicles did not contain significantly larger oocytes than Ki67-negative follicles, on days 12 or 21 (Fig. 6B). Furthermore, Ki67-positive primordial follicles did not have significantly more GCs than negative follicles on either day (Fig. 6C).

We went on to examine the relationship between the Ki67 labelling index and further oocyte growth in follicles at all stages. Considering all GCs, flat and cuboidal, the proportion of labelled cells remained low (<10%) during a period of considerable oocyte growth, up to 30 μm in diameter (an eightfold increase in oocyte volume). Between 30 and 40 μm in diameter there was a dramatic increase in the labelling index and levels of Ki67 immunolabelling remained high with subsequent oocyte growth (Fig. 7A, dotted line). Initially we interpreted this as being due to the increase in the proportion of cuboidal cells with increasing oocyte size (supplementary material Fig. S1), cuboidal cells having a higher labelling index than flat cells (Fig. 5A). However, limiting our analysis to just cuboidal cells, we saw a similar trajectory, with an initial low labelling index that increased after the oocyte reached 30 μm in diameter (Fig. 7A, continuous lines).

To further investigate what changes were occurring in the follicle at this point, we explored the relationship between oocyte growth and the number of GCs in individual follicles at specific stages of follicle development. On both day 12 and 21 there was a low but steady increase in GC number up to the primary stage. With the development of the second layer of GCs a significant change in the relationship between the number of GCs and oocyte growth occurred (Fig. 7B; supplementary material Fig. S1). This prompted us to investigate whether GCs divided more as they lost contact with the basal lamina. We found that the proportion of Ki67-positive GCs in the inner layers was significantly higher than the proportion on the basal lamina (Fig. 7C,D).

Formation of multiple layers of GCs

During our examination of the follicles it appeared that the GCs became closely packed on the basal lamina when the second layer of GCs was forming. This, coupled with our observations of decreased Ki67 immunolabelling in basal cells, led us to ask whether the basal lamina has a role in regulating the onset of the formation

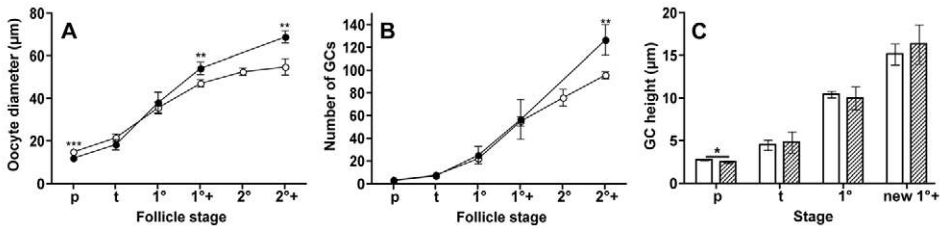

Fig. 3. (A-C) Growth trajectory of follicles during initiation of follicle growth. Oocyte diameter (A), number of GCs (B) and GC height (C) in the largest cross section on days 12 (open circles and white bars) and 21 (black circles, hatched bars); p, primordial; t, transitional; 1°, primary; 1°+, primary with a second layer forming; 2°, secondary; 2°+, secondary with third layer forming; new 1°+, primary with < five second-layer cells. Values are presented as the mean ± 95% confidence interval. *** $P<0.0001$, ** $P<0.01$ and * $P<0.05$: significant differences between days 12 and 21. For all three variables there was a significant difference between values at successive stages (supplementary material Table S1), except oocyte diameter between 2° to 2°+ on day 12.

of a second layer of GCs. To give an estimate of packing density, we calculated how 'wide', on average, the GCs were on the basal lamina, and compared the packing density of GCs at each developmental stage. For this analysis we subdivided the primary plus category into those follicles which were just starting to develop a second layer (termed 'new second layer'), and those with a more extensive second layer ('established second layer'). The mean width of GCs was similar at each stage on day 12 and day 21, therefore the data were amalgamated for further analysis. There was a significant reduction in the mean width of GCs on the basal lamina from the primordial stage to the transitional and primary stages (Fig. 8A). At these earliest stages there was a wide range of GC widths, the variance of which reduced significantly as follicles progressed from primordial to transitional (P<0.0001), and from transitional to primary (P<0.0001) stages. The variance was similar as new

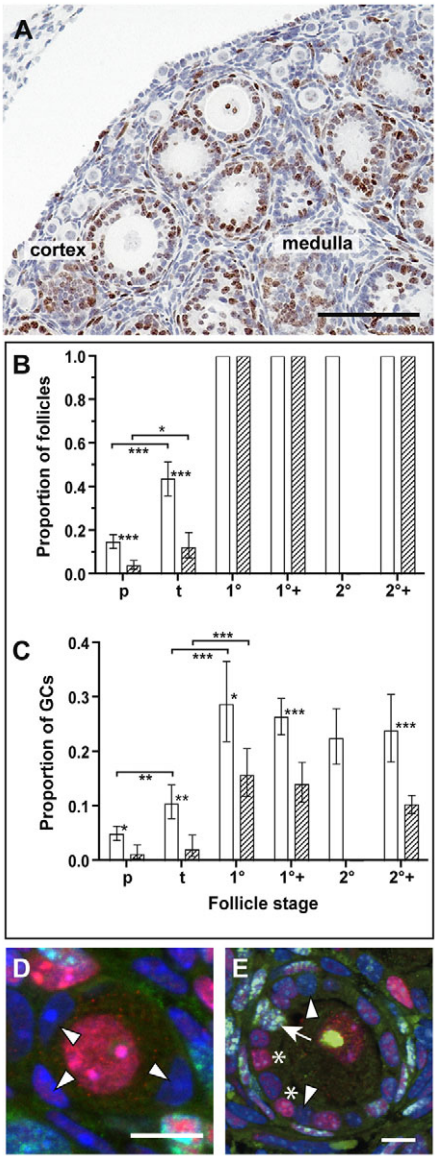

Fig. 4. Ki-67 immunolabelling of follicles. (A) Low-magnification view of day 12 ovary immunolabelled for Ki67 (brown) showing widespread labelling of GCs that is increased in larger follicles. Scale bar, 100 µm. (B,C) Proportion of follicles with one or more Ki67-positive GCs (B) and proportion of Ki67-positive GCs on days 12 (open bars) and 21 (hatched bars) (C). p, primordial; t, transitional; 1°, primary; 1°+, primary with a second layer forming; 2°, secondary; 2°+, secondary with third layer forming. Values are means and 95% confidence interval. Asterisks on the right shoulder of the day 12 bars denote significant differences between days 12 and 21, asterisks on horizontal lines mark significant differences between stages; *** P<0.0001, ** P<0.01, * P<0.05. In B, differences between transitional and primary, and between subsequent stages, are impossible to compare by regression when the proportion =1. (D) Primordial follicle with unlabelled GCs (arrowheads). Scale bar, 10 µm. (E) Primary follicle immunolabelled for Ki67 (green) and MCM2 (red), with nuclei labelled with DAPI (blue). Nuclei indicated by asterisks are MCM2-positive, nucleus indicated by white arrow is Ki67- and MCM2-positive; white arrowheads indicate Ki67- and MCM2-negative nuclei (DAPI only). Scale bar:10 µm.

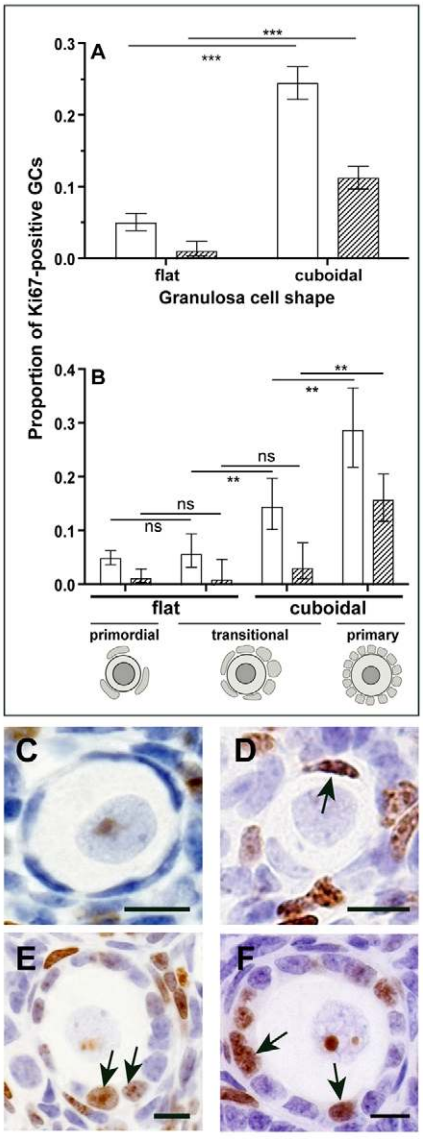

Fig. 5. Relationship between GC shape and Ki67 immunolabelling. (A) Proportion of flat and cuboidal GCs that are Ki67-positive on days 12 (open bars) and 21 (hatched bars). (B) Proportion of flat and cuboidal GCs that are Ki67-positive at the primordial, transitional and primary stages, on days 12 and 21. Values are presented as the mean ± 95% confidence interval. *** P<0.0001, ** P<0.01, * P<0.05: significant differences between days 12 and 21. (C) High-magnification view of primordial follicle with no Ki67-positive GCs. (D) Ki67-positive primordial follicle with labelled flat GC (arrowed). (E,F) Ki67-positive transitional (E) and primary (F) follicles with labelled cuboidal cells (examples indicated by arrows). Scale bars: 10 µm.

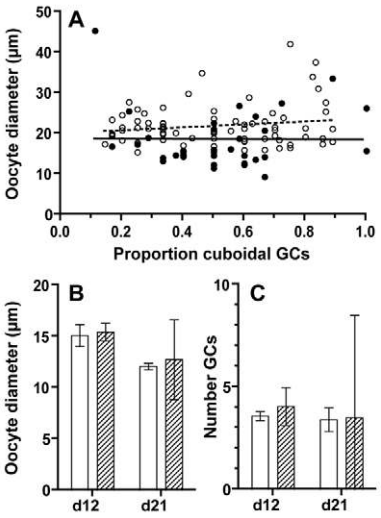

Fig. 6. (A) Oocyte diameter and proportion of cuboidal cells in transitional follicles on days 12 (open circles, dotted line) and 21 (filled circles, continuous line). Lines are linear regression fits with no significant slope and no difference between days 12 and 21. (B,C) Oocyte diameter (B) and number of GCs (C) are similar in Ki67-negative (open bars) and Ki67-positive (hatched bars) primordial follicles on days 12 and 21. Values are presented as the mean ± 95% confidence interval.

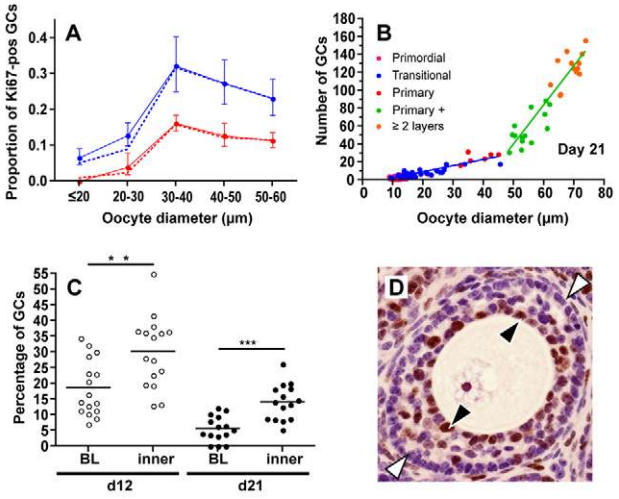

Fig. 7. (A) Increasing proportion of Ki67-positive GCs with increasing oocyte diameter on days 12 (blue) and 21 (red). Dotted lines are for all GCs, continuous lines are for just cuboidal GCs. Values are presented as the mean ± 95% confidence interval. (B) Relationship between oocyte diameter and the number of GCs on day 21. Lines are linear regression fits of unilaminar (blue line) and multilayered (green line) follicles. For day 12 see supplementary material Fig. 1B. (C) Percentage of Ki67-positive GCs on the basal lamina (BL) and inner layers (inner) on days 12 and 21. (D) Day 21 follicle at the secondary-plus stage with sparse Ki67 labelling on the basal lamina (white arrowheads), and more on the inner layers (black arrowheads).

layers were added (P=0.66). With the appearance of second and subsequent layers, the GCs attained (and maintained) a maximal packing density on the basal lamina of around one GC per 6 μm of basal lamina (Fig. 8A). As GCs became narrower, they became taller (Fig. 8B).

We went on to examine the ultrastructural appearance of the basal lamina at these early stages and to investigate whether it changed during formation of multiple layers (Fig. 8C-G). In unilaminar follicles, the basal lamina was generally straight, with a single layer of lamina densa, although this was not always well defined in follicles at this stage (Fig. 8C,D). Outside the lamina densa, away from the GCs, there were occasional collagen fibrils visible (Fig. 8D), but this layer was not continuous or extensive and, indeed, on day 12 was frequently absent. With the appearance of a second layer of GCs, the lamina densa was either straight or closely followed indentations in the GCs, with occasional extra layers of the lamina densa seen on the theca side (Fig. 8E). In follicles with multiple layers of GCs the layer of collagen fibrils varied from sparse to thick and dense (Fig. 8F,G). Hemidesmosomes were attached to the lamina densa by anchoring fibrils (Fig. 8E, insert).

The appearance of collagen fibrils outside the lamina densa led us to consider whether the surroundings of the follicle have a role in providing a confined area for GCs to become packed upon. This was supported by our observations of strong actin labelling within the theca cells, which appeared to form a mesh around the follicle and was strikingly aligned to the basal lamina (Fig. 8H).

Orientation of GC mitosis

The above described observations prompted us to examine whether the attainment of a maximal packing density on the basal lamina was accompanied by a change in the orientation of mitoses (Fig. 9). Approximately 150 H&E-stained sections of day 12 and day 21 ovaries were examined for mitoses in the GCs, and ~100 mitotic figures with a clear orientation were found (Table 2). No mitotic figures were seen in primordial follicles. All of the five mitoses in transitional follicles were, as expected, oriented parallel to the oocyte surface (Fig. 9Ai; Fig. 9B). As the GCs changed shape a mixture of mitoses that were parallel or perpendicular to the basal lamina and oocyte surface were seen (Fig. 9Aii; Fig. 9C; Table 2). The key observation was in the primary plus follicles, where many columnar GCs are attached at the basal surface to the basal lamina via hemidesmosomes, and at the opposite apical surface to the oocyte via TZP and gap junctions (described as 'span basal-lamina-oocyte' in Table 2; Fig. 9Aiii). The vast majority (94%) of the mitotic figures in these cells were perpendicular to the basal lamina (Fig. 9D). This type of perpendicular cell division will result in one daughter cell remaining attached to the basal lamina (Fig. 9Aiv), and the other losing contact and contributing to the new second layer of GCs next to the oocyte (Fig. 9Av). These new inner daughter cells appear to be initially evenly and sparsely scattered around the oocyte (Fig. 2E), with the inner layer becoming more continuous, probably as a result of both inward-oriented division from cells on the basal lamina (Fig. 9Avi; Fig. 9F), and lateral division of new inner cells (Fig. 9G). With the development of more layers of GCs, cells divide perpendicular (Fig. 9F), parallel (Fig. 9G), and obliquely to the basal lamina and/or the oocyte.

Discussion

During initiation of follicle growth, GCs change shape from flattened to cuboidal, then columnar. Here we have shown quantitatively that as the cells become cuboidal their proliferation rate increases. Columnar GCs are polarised, with the nucleus lying adjacent to the basal lamina. Cells become three to four times narrower, and sixfold taller, and become more densely packed on the basal lamina. As a second layer of GCs starts to develop, GCs reach a maximal packing density on the basal lamina that is

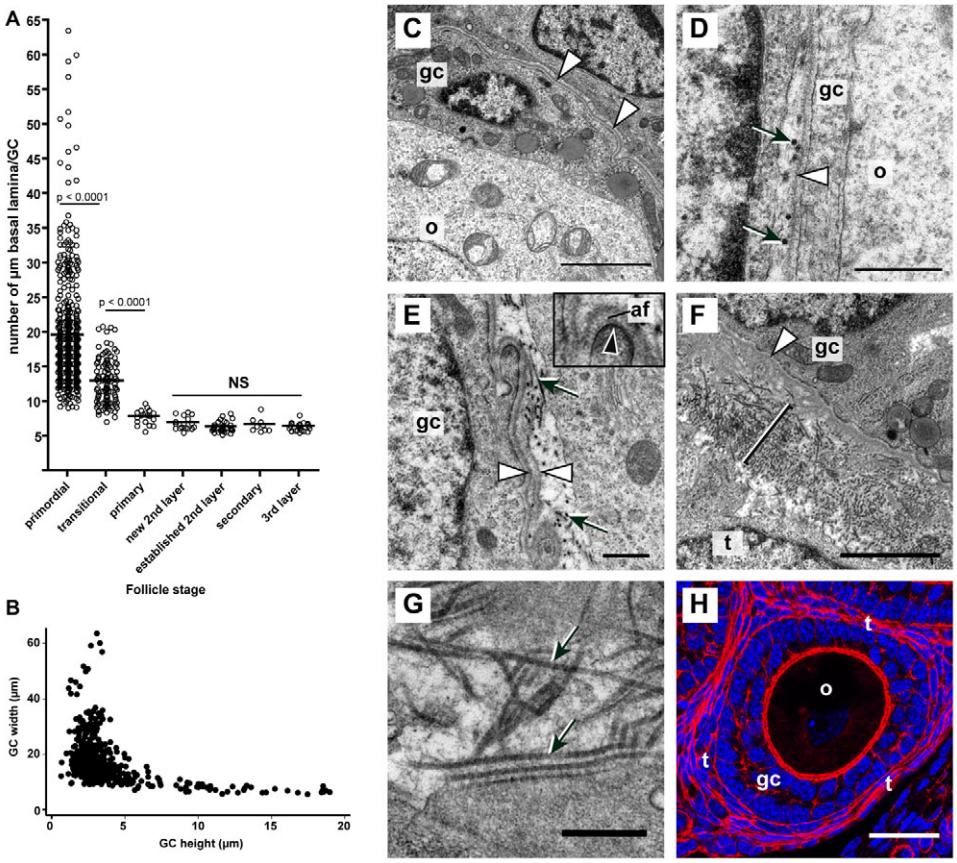

Fig. 8. (A) Scattergram of widths of GCs on basal lamina on both day 12 and 21. Note reduction of widths from primordial to primary stage. Significant differences between means (horizontal lines) are marked. (B) Scattergram of GC width against GC height in follicles from primordial to the 'new second layer' stage on both day 12 and 21. (C-G) Electron micrographs of basal lamina; gc, granulosa cell; o, oocyte; t, theca cell; white arrowheads indicate lamina densa; black arrowheads indicate hemidesmosomes; black arrows indicate collagen fibrils. (C) Day 21 primordial follicle. Note clear lamina densa (arrowheads). Scale bar: 2 µm. (D) Day 10 primordial follicle. Note occasional and sparse collagen fibrils (arrows). Scale bar: 500 nm. (E) Day 10 follicle at the primary plus stage. Basal lamina closely following GC indentations. Occasional multiple layers of lamina densa are visible (arrowheads), as are anchoring filaments (af) between hemidesmosome (black arrowhead) and lamina densa (see insert). Note more numerous collagen fibrils (arrows). Scale bar: 500 nm. (F) Day 21 multilayered follicle. Note thick layer of collagen fibrils (square bracket). Bar: 2 µm. (G) High power of collagen fibrils surrounding a day 21 primary follicle. Scale bar: 500 nm. (H) F-actin expression (red) in a day 21 primary-plus follicle, note strong cortical staining in theca cells. Nuclei are blue (DAPI). Scale bar: 30 µm.

maintained with the development of further layers. The formation of a second layer of GCs results from basal cells changing their mitotic spindle orientation, so that they divide inwards, with the new layer forming on the inner aspect of the basal GC layer, next to the oocyte. The change in spindle orientation is probably caused by a combination of the GCs becoming tightly packed, and the columnar cells being tethered at opposite ends to the basal lamina and the oocyte. These observations suggest that the basal lamina does not expand indiscriminately with cell division but, in conjunction with the enveloping layer of collagen fibrils and the actin-rich theca layer, imposes some restraint, thereby promoting the formation of a second layer of GCs.

Flat GCs can proliferate but rarely do so, particularly in older mice. Cuboidalisation of cells results in a fivefold increase in proliferation, as demonstrated by an increased Ki67 labelling index and an increase in GC number in transitional and primary follicles. These observations are in contrast to in vitro studies of non-transformed endothelial cells, showing that flattened cells have the greater proliferative capacity, which decreases as the cells become more cuboidal, become confluent and ultimately undergo contact inhibition (Chen et al., 1997; Folkman and Moscona, 1978). However, we also observed a subsequent decline in proliferation as GCs reach a maximal packing density, suggesting that a degree of contact inhibition occurs in GCs on the basal lamina. This has been illustrated by a decline in both Ki67 immunolabelling and in the number of mitotic figures in basal cells; only four (13%) of the 30 mitotic figures observed in follicles with two or more layers were on the basal lamina. A low number of mitotic figures have also been observed in GCs on the basal lamina in bovine antral follicles, with the highest numbers being observed in the middle layers (van Wezel et al., 1999).

The potential for flat GCs to occasionally divide has been described before, although not specifically quantified. Positive immunostaining for PCNA has been observed occasionally in primordial follicles of cow, primate, human and sheep (Gougeon and Busso, 2000; Lundy et al., 1999; Wandji et al., 1997; Wandji et al., 1996) but not rat (Gaytan et al., 1996; Oktay et al., 1995). However, positive labelling of flattened GCs following long term in vivo infusion of rats with [^{3}H]thymidine (Hirshfield, 1989) or BrdU (Meredith et al., 2000) suggested that very low levels of cell division were occurring. It is generally thought that primordial follicles are quiescent, but several studies have challenged this notion (Hirshfield, 1989; Lundy et al., 1999; Stubbs et al., 2007). Our results support the view that not all primordial follicles are entirely 'quiescent', and that cuboidalisation of GCs is not an absolute pre-requisite for entry into the cell cycle.

Our observations of GCs that were not labelled when staining for either Ki67 or MCM2 (which labels cells in the cell cycle) in early preantral follicles further demonstrate that not all the GCs remain in the cell cycle, even a prolonged one, and suggests that these cells are in G0. Prolonged persistence of BrdU labelling in transitional rat follicles for more than 150 days supports this suggestion that GCs at these early stages can enter and leave the cell cycle (Meredith et al., 2000).

A decline in GC proliferation with advancing age has previously been reported in mice (Pedersen, 1969), monkeys (Gougeon and Busso, 2000), sheep (Lundy et al., 1999) and rats (Hirshfield, 1985). As the numbers of GCs at successive stages of early follicle

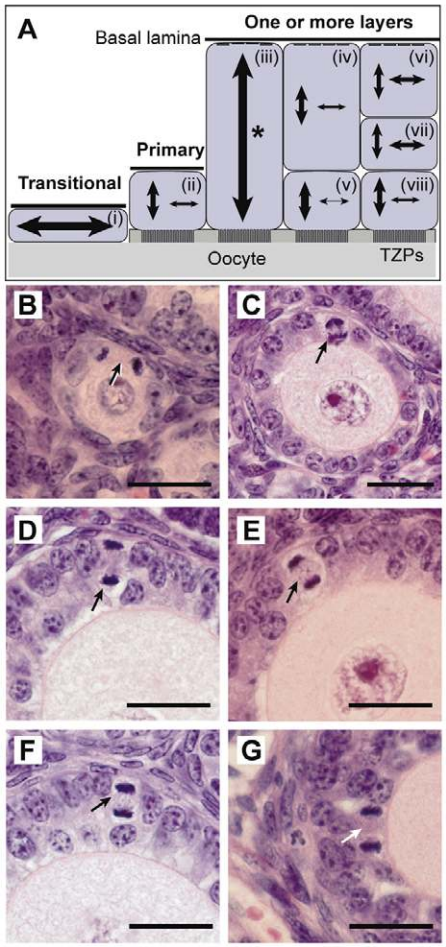

Fig. 9. (A) Diagram illustrating axes of mitoses at different stages of follicle development and in different layers of the GCs. Thicker lines mark predominant angle. (B-G) H&E stained sections of day 12 (B, C, E–F) and 21 (D) ovary showing angle of mitoses (arrows). (B) Mitosis parallel to basal lamina and oocyte surface in transitional follicle. (C) Mitosis perpendicular to basal lamina and oocyte surface in primary follicle. (D and E) Perpendicular mitosis in GC spanning between GC and oocyte. (F) Perpendicular mitosis in a basal GC. (G) Mitosis in an inner GC parallel to oocyte surface. Scale bars: 20 μm.

development were similar on days 12 and 21, the significantly lower proportion of Ki67-positive GCs on day 21 suggest that follicle development becomes slower as the mice reach adulthood. The lower levels of Ki67 immunolabelling on day 21 might be due to the presence of larger preantral and antral follicles, which are sources of possible inhibitors of growth of smaller follicles, such as anti-Müllerian hormone (Durlinger et al., 2002) or activin (Mizunuma et al., 1999). Alternatively, it is possible that increased GC proliferation is due to increased levels of plasma follicle stimulating hormone (FSH) that is seen in prepubertal mice and peaks between days 10 and 16 (Dullaart et al., 1975; Halpin et al., 1986; Stiff et al., 1974), before declining to adult levels. This is feasible, because FSH-receptor mRNA is present in GCs from just after birth in mice (O'Shaughnessy et al., 1996), with levels peaking on day 10 pp (O'Shaughnessy et al., 1997), and FSH has been directly shown to stimulate GC proliferation in preantral follicles (Kreeger et al., 2005; Roy and Greenwald, 1989).

It is clear that bi-directional communication between the oocyte and the surrounding GCs is crucial for successful follicle development (Eppig, 2001; Gilchrist et al., 2004a; Matzuk et al., 2002). However, it is significant that the oocytes in Ki67-negative and -positive primordial follicles are similar in size, indicating that the onset of GC division (as measured by Ki67 immunolabelling) is not directly associated with the onset of oocyte growth. This is consistent with the reported lack of association between PCNA labelling and oocyte size in sheep primordial follicles (Lundy et al., 1999). Furthermore, to our surprise, we saw no increase in oocyte size as the proportion of cuboidal cells increased in transitional follicles. These observations suggest that early events in the oocyte and GCs could be occurring independently, but in parallel.

It is interesting that the relationship between GC proliferation and oocyte growth changed with the development of the second layer of GCs. In the unilaminar follicle, all the GCs are in contact with the basal lamina on one side and the oocyte on the other. With the onset of GC multilayering, two new populations of GCs develop; one in contact with the oocyte, the other with the basal lamina. Subsequent inner layers will be in contact with neither. The observation of a higher Ki67 labelling index in inner cells suggests that cells that have lost contact with the basal lamina divide more frequently, with the removal of the physical and signalling constraints imposed by contact with this ECM. Alternatively, the oocyte might be producing a factor that stimulates proliferation. It is notable that follicles in mice that lack the oocyte-specific growth factor Gdf9 fail to develop a second layer of GCs and have lower levels of GC proliferation, although oocyte growth continues (Dong et al., 1996; Elvin et al., 1999b). It is possible that Gdf9, which first appears at the primary stage (Dong et al., 1996; Elvin et al., 1999a), and increases GC proliferation in vitro (Gilchrist et al., 2004b), is producing a local gradient and stimulating proliferation close to the oocyte. Localised gradients of oocyte-derived BMPs have been observed previously (Hussein et al., 2005).

In follicles that started to develop a second layer, lateral proliferation was not observed in cells contacting both the basal lamina and the oocyte, and the vast majority (94%) of mitoses were oriented perpendicular to the basal lamina. Perpendicular mitoses have been observed in the basal layer of the epidermis and are thought to result both in stratification and asymmetric cell divisions, with one daughter cell losing contact with the basal lamina and therefore losing basal cell characteristics (Lechler and Fuchs, 2005). Furthermore, the orientation of the mitosis is regulated by cell shape, with the axis of the mitosis lying parallel to the long axis of the cell (O'Connell and Wang, 2000). Indeed, it is becoming clear that the cortical landmarks laid down by the distribution of adhesive contacts and external forces have a key role in defining the orientation of the mitotic spindle, and the spindle is aligned along the traction field defined in the preceding interphase (Thery and Bornens, 2006). It is clear from our EM studies, and the work of others, that in unilaminar follicles GCs are tethered at both ends, one end to the lamina densa by anchoring filaments, and the other end to the oocyte via TZPs (Albertini et al., 2001) and adhesive junctions (Fair et al., 1997; Zamboni, 1974). These opposing attachments could produce a traction field along the length of the columnar GC, that would orient the mitotic spindle perpendicular to the basal lamina, producing two asymmetric daughter cells, one basal and one inner. In-situ hybridisation analysis of ovaries from adult mouse chimaeras made by aggregating wild-type and β-globin transgenic eight-cell embryos demonstrated radial proliferation of GC clones across the follicle wall, supporting the idea that mitosis

Table 2. Angle of mitoses relative to the basal lamina

Stage	Position*	Number		Angle relative to basal lamina/oocyte		
		Mitoses	Follicles	Perpendicular	Parallel	Oblique
Primordial		0	0	–	–	–
Transitional		5	5	0 (0%)	5 (100%)	0
Primary		14	13	9 (64%)	4 (29%)	1 (7%)
1° plus†	Span BL-oocyte	37	55	35 (94%)	1 (3%)	1 (3%)
	BL	13		8 (62%)	4 (31%)	1 (8%)
	Inner	18		14 (78%)	3 (17%)	1 (6%)
≥2 layers	BL	4	25	2 (50%)	2 (50%)	0 (0%)
	Inner	26		14 (54%)	7 (27%)	5 (19%)
Total		117	98	82	26	9

*Position relative to follicle: span BL-oocyte, GC abutting both the basal lamina and the oocyte; BL, on basal lamina; inner, not on basal lamina.
†Primary stage with second layer forming.
Numbers in parentheses indicate the percentage of mitoses.

perpendicular to the basal lamina is important in the formation of multiple layers (Boland and Gosden, 1994).

The basal lamina appears to be crucial for normal folliculogenesis and the development of multiple layers. Mice that lack the gene encoding the forkhead transcription factor Foxl2 lack a continuous, regular, basal lamina around follicles and fail to form follicles with multiple layers of GCs (Uda et al., 2004). ECM provides a scaffold for cells, affecting cell behaviour by both its protein composition and physical stiffness or rigidity, and altering cell binding, cortical cues and downstream signalling from the junctions (Berrier and Yamada, 2007; Black et al., 2008). The protein composition of basal lamina changes during folliculogenesis owing to the varying presence and proportions of isoforms of type IV collagen and laminin (Rodgers et al., 2003). In the mouse ovarian follicle, type-IV collagen has been shown to be undetectable by immunohistochemistry in the basal laminae of primordial follicles and to increase as the follicle develops (Berkholtz et al., 2006a). The collagen-laminin composition of the ECM can regulate GC proliferation, with collagen being inhibitory (Huet et al., 2001; Oktay et al., 2000), thus the appearance of collagen IV in the basal lamina might inhibit GC proliferation in adjacent cells.

The physical stiffness of the basal lamina itself and of the surrounding cells might also be involved in constraining lateral cell division in the basal GCs. Mechanical signals can be transmitted bi-directionally between the ECM and the cytoskeleton via transmembrane integrins, resulting in changes in the ECM (rigidity, matrix deposition and remodelling) or the cell (shape, cytoskeletal rigidity, signalling) (Berrier and Yamada, 2007; Ingber, 2004). It has recently been elegantly demonstrated that the stiffness or rigidity of the environment can regulate follicle growth, with isolated mouse follicles cultured in gels of increasing concentrations of alginate (and hence rigidity) exhibiting reduced follicle growth (Xu et al., 2006). Furthermore, we observed collagen fibrils surrounding the basal lamina. These collagen fibrils were similar to those associated with the lamina densa of epithelia in exocrine glands, which contribute to connective tissue and provide mechanical support (Hosoyamada and Sakai, 2003). Collagen is stiff and almost inextensible (Black et al., 2008), so it can be envisaged that collagen fibrils surrounding the follicle could provide mechanical constraint, which could be enhanced by the extensive actin expression observed in the overlying theca layer. The theca-cell layer can expand in a regulated manner, as shown by the presence of mitoses and Ki67-positive cells.

In summary, we have shown that the early ovarian follicle provides a new model for studying the relationship between epithelial cell shape, attachment to the basal lamina and cell behaviour. Oocytes in primordial follicles are enveloped in flat cells that rarely divide. In response to an as yet unknown signal, the GCs cuboidalise and divide more frequently, reaching a maximal packing density on the basal lamina, such that cells are compelled to divide inwards to produce a second layer. We propose that the basal lamina, collagen fibrils and theca-cell layer provide mechanical constraint around the follicle to promote packing of the GCs on the basal lamina and the subsequent formation of multiple layers, while being able to expand in a regulated manner as the follicle grows. Thus, change in cell shape has a key role in initiation of follicle growth.

Materials and Methods

Ovary preparation

Whole ovaries were collected from female C57BL/6 mice pups (Harlan Olac Ltd, Bicester, Oxon, UK) killed by cervical dislocation at days 12 and 21 post partum. Mice were housed in accordance with the Animals (Scientific Procedures) Act of 1986 and associated Codes of Practice.

Ovaries were fixed in 10% buffered formalin (VWR International, Leicestershire, UK) for immunohistochemical or immuofluorescence analysis, or Bouin's fixative (Sigma-Aldrich Ltd., Poole, Dorset, UK) for morphological analysis. All ovaries were dehydrated, processed and embedded in paraffin before being serially sectioned at a thickness of 5 μm. Further ovaries were fixed in 4% paraformaldehyde, infiltrated with 30% sucrose and frozen in optimal cutting temperature (OCT) compound before cryostat sectioning.

Transmission electron microscopy

Ovaries were fixed for 24 hours in 3% v/v glutaraldehyde in 0.1 M cacodylate buffer (pH 7.2), post-fixed in 1% osmium tetroxide in cacodylate buffer for 1 hour and embedded in araldite. Ultrathin sections were stained in a saturated solution of uranyl acetate in 50% ethanol, followed by Reynold's lead citrate, and examined with a Philips CM10 electron microscope.

Immunohistochemistry for Ki67

Immunohistochemistry was performed as described recently (Stubbs et al., 2005), using a rabbit serum block. Sections were incubated with a monoclonal antibody against Ki67 (1:50, DakoCytomation Ltd., Ely, UK; M7249, clone TEC-3) in blocking solution overnight at 4°C, followed by a 1-hour incubation in a secondary biotinylated rabbit anti-rat antibody (1:200, DakoCytomation Ltd; E0468) at room temperature. Labelling was visualised as previously described (Stubbs et al., 2005). As a negative control the primary antibody was omitted.

Immunofluorescence for β-catenin, actin, Ki67 and MCM2

Dehydration and antigen retrieval of formalin-fixed sections were as described previously (Stubbs et al., 2005) before incubation with primary antibodies against either β-catenin (prediluted, Abcam, Cambridge, UK, ab15180) or a cocktail of Ki67 (as above) and MCM2 (1:100, Abcam; ab31159) overnight at 4°C, followed by a 1-

hour incubation in a 1:200 dilution of appropriate secondary antibodies conjugated with either Alexa-Fluor-633 (Molecular Probes, Eugene, OR, USA) for detection of β-catenin, or a mixture of Alexa-Fluor-488 and Alexa-Fluor-555 (Molecular Probes) for the detection of Ki-67 and MCM-2, respectively. F-actin was localised in frozen sections by a 90-minute incubation in Alexa-Fluor-555 phalloidin (A34055, Molecular Probes). Following a brief (1-minute) wash in 1 μg/ml DAPI (Sigma-Aldrich) in water, slides were mounted with Prolong Gold antifade reagent with DAPI (Invitrogen, Paisley, UK) and analysed using a confocal laser-scanning microscope (Leica SP2).

Analysis of Ki67 immunolabelling

Slides were examined on an E600 microscope (NikonUK Ltd., Kingston-upon-Thames, UK) and digital images were captured with a DXM 1200 digital camera (Nikon) using the Lucia image analysis program (Nikon). Follicles were scored for developmental stage on the basis of GC shape and the number and completeness of GC layers, as follows: (1) primordial, with one layer of flattened pre-GCs; (2) transitional, where at least one but not all GCs were cuboidal; (3) primary, with one complete layer of cuboidal GCs; (4) primary plus, with an incomplete second layer of GCs; (5) secondary, with two complete layers of GCs and (6) secondary plus, with two complete layers overlying some of the oocyte and three or four layers over the rest (Fig. 1B).

Follicles containing an oocyte with a sharply demarcated nuclear membrane and/or nucleolus were considered to have been sectioned at their largest cross section (LCS) and were analysed in detail. Oocyte and follicle diameters were calculated from the mean of two perpendicular measurements made at the LCS, using Lucia (Nikon). Oocyte diameter excluded the zona pellucida. The boundary of the follicle was defined as the basement membrane, clearly visible as a delineation between the GCs and the surrounding stroma/theca (Fig. 1C).

Unilaminar follicles were scored for GC shape (flattened or cuboidal), number (number of GC nuclei) and Ki67-positivity (moderate or strong brown staining) in follicles at the microscope (×60 objective), while focusing up and down. Follicles with multiple layers of GCs were analysed from digital images. The proportion of Ki67-positive GCs determined the labelling index of the follicle. In a few (seven) follicles, the follicle boundary was not clear for the entire circumference, and in these cases the number of GCs was not counted. To quantify change in GC shape, the average GC height for each follicle was calculated by subtracting the oocyte radius from the follicle radius. GC height, therefore, included developing zona pellucida.

Packing density of GCs on basal lamina

To analyse packing density of GCs on the basal lamina, follicles were categorised as described above, but the primary plus category was subdivided into 'new second layer', where follicles had between one and five GCs in the second layer, and 'established second layer', where follicles had a second layer of more that five GCs, which was not yet complete. To estimate the packing density of GCs the circumference of the each follicle (which was considered to represent of the amount of basal lamina in the LCS) was calculated from the follicle diameter (πD). The number of GCs in contact with the basal lamina was counted, and the average 'width' of GCs calculated (follicle circumference/number of GCs on basal lamina). In addition, the number of Ki67-positive GCs on the basal lamina was counted.

Orientation of mitoses

Bouin's-fixed ovaries were serially sectioned and mounted on slides. Every fifth slide was stained conventionally with haematoxylin and eosin. Every section was examined and digital images captured of follicles with GCs undergoing mitosis (×60 objective). In the majority of follicles, it was possible to classify the orientation of the mitotic spindle relative to the oocyte surface and basal lamina (perpendicular or parallel) from the orientation of either the metaphase plate or spindle itself, or the relative positions of separating chromatids at anaphase or telophase.

Statistical analysis

Statistical analysis of Ki67 staining of GC nuclei was carried out using Stata 10 for Macintosh (Stata Corporation, College Station, TX). The effect of both follicle stage and pup age on oocyte diameters, GC heights and the numbers of GCs in the LCS of follicles was analysed using ordinary regression (regress command), using robust standard errors with clustering by pup. This takes account of possible within-pup correlation in follicle development. Pair-wise comparisons (for example, comparison of oocyte diameter at the primordial stage between day 12 and day 21) were corrected for multiple comparisons by multiplying the P value by the number of comparisons made. A few groups were not normally distributed and significant differences were confirmed using non parametric analysis (Kruskal Wallis for multiple groups; if $P<0.05$, pair-wise comparisons were performed using the Mann-Whitney U test, again correcting for multiple comparisons).

Mean proportions of both Ki67-positive follicles (with one or more positive GCs) and Ki67-positive GCs at each stage of development and at each age were computed and compared using binomial regression (binreg command). For comparisons between proportions of follicles, confidence intervals and P values in different groups were computed using robust standard errors with clustering by pup. This takes account of possible within-pup correlation in Ki67 staining. For comparisons between proportions of GCs, confidence intervals and P values in different groups were computed using robust standard errors with clustering by follicles, thus taking into account possible within-follicle correlation of dividing cells in those follicles which have initiated growth. P values were corrected for multiple comparisons at each stage of follicle development.

When investigating the density of GCs on the basal lamina, the variance of the width of the GCs lying on the basal lamina was compared at each stage using Levene's robust test statistic for equality of variances (robvar command).

We acknowledge the support of BBSRC grants BB/C514274/1 (P.D.S.-B.) and BB/F000014/1 (J.M.M.), and of a Health Foundation Student Research Fellowship (G.S.J.). We also thank Angelos Skodras (Institute of Reproductive and Developmental Biology) and Martin Spitaler (F.I.L.M. Unit, Imperial College London) for help with the confocal microscopy.

References

Albertini, D. F., Combelles, C. M., Benecchi, E. and Carabatsos, M. J. (2001). Cellular basis for paracrine regulation of ovarian follicle development. *Reproduction* **121**, 647-653.

Berkholtz, C. B., Lai, B. E., Woodruff, T. K. and Shea, L. D. (2006a). Distribution of extracellular matrix proteins type I collagen, type IV collagen, fibronectin, and laminin in mouse folliculogenesis. *Histochem. Cell Biol.* **126**, 583-592.

Berkholtz, C. B., Shea, L. D. and Woodruff, T. K. (2006b). Extracellular matrix functions in follicle maturation. *Semin. Reprod. Med.* **24**, 262-269.

Berrier, A. L. and Yamada, K. M. (2007). Cell-matrix adhesion. *J. Cell Physiol.* **213**, 565-573.

Black, L. D., Allen, P. G., Morris, S. M., Stone, P. J. and Suki, B. (2008). Mechanical and failure properties of extracellular matrix sheets as a function of structural protein composition. *Biophys. J.* **94**, 1916-1929.

Boland, N. I. and Gosden, R. G. (1994). Clonal analysis of chimaeric mouse ovaries using DNA in situ hybridization. *J. Reprod. Fertil.* **100**, 203-210.

Burns, K. H., Owens, G. E., Fernandez, J. M., Nilson, J. H. and Matzuk, M. M. (2002). Characterization of integrin expression in the mouse ovary. *Biol. Reprod.* **67**, 743-751.

Chen, C. S., Mrksich, M., Huang, S., Whitesides, G. M. and Ingber, D. E. (1997). Geometric control of cell life and death. *Science* **276**, 1425-1428.

Dong, J., Albertini, D. F., Nishimori, K., Kumar, T. R., Lu, N. and Matzuk, M. M. (1996). Growth differentiation factor-9 is required during early ovarian folliculogenesis. *Nature* **383**, 531-535.

Dullaart, J., Kent, J. and Ryle, M. (1975). Serum gonadotrophin concentrations in infantile female mice. *J. Reprod. Fertil.* **43**, 189-192.

Durlinger, A. L., Gruijters, M. J., Kramer, P., Karels, B., Ingraham, H. A., Nachtigal, M. W., Uilenbroek, J. T., Grootegoed, J. A. and Themmen, A. P. (2002). Anti-Mullerian hormone inhibits initiation of primordial follicle growth in the mouse ovary. *Endocrinology* **143**, 1076-1084.

Elvin, J. A., Clark, A. T., Wang, P., Wolfman, N. M. and Matzuk, M. M. (1999a). Paracrine actions of growth differentiation factor-9 in the mammalian ovary. *Mol. Endocrinol.* **13**, 1035-1048.

Elvin, J. A., Yan, C., Wang, P., Nishimori, K. and Matzuk, M. M. (1999b). Molecular characterization of the follicle defects in the growth differentiation factor 9-deficient ovary. *Mol. Endocrinol.* **13**, 1018-1034.

Eppig, J. J. (2001). Oocyte control of ovarian follicular development and function in mammals. *Reproduction* **122**, 829-838.

Fair, T., Hulshof, S. C., Hyttel, P., Greve, T. and Boland, M. (1997). Oocyte ultrastructure in bovine primordial to early tertiary follicles. *Anat. Embryol.* **195**, 327-336.

Folkman, J. and Moscona, A. (1978). Role of cell shape in growth control. *Nature* **273**, 345-349.

Gaytan, F., Morales, C., Bellido, C., Aguilar, E. and Sanchez-Criado, J. E. (1996). Proliferative activity in the different ovarian compartments in cycling rats estimated by the 5-bromodeoxyuridine technique. *Biol. Reprod.* **54**, 1356-1365.

Gilchrist, R. B., Ritter, L. J. and Armstrong, D. T. (2004a). Oocyte-somatic cell interactions during follicle development in mammals. *Anim. Reprod. Sci.* **82-83**, 431-446.

Gilchrist, R. B., Ritter, L. J., Cranfield, M., Jeffery, L. A., Amato, F., Scott, S. J., Myllymaa, S., Kaivo-Oja, N., Lankinen, H., Mottershead, D. G. et al. (2004b). Immunoneutralization of growth differentiation factor 9 reveals it partially accounts for mouse oocyte mitogenic activity. *Biol. Reprod.* **71**, 732-739.

Gougeon, A. and Busso, D. (2000). Morphologic and functional determinants of primordial and primary follicles in the monkey ovary. *Mol. Cell. Endocrinol.* **163**, 33-42.

Halpin, D. M., Jones, A., Fink, G. and Charlton, H. M. (1986). Postnatal ovarian follicle development in hypogonadal (hpg) and normal mice and associated changes in the hypothalamic-pituitary ovarian axis. *J. Reprod. Fertil.* **77**, 287-296.

Hirshfield, A. N. (1985). Comparison of granulosa cell proliferation in small follicles of hypophysectomized, prepubertal, and mature rats. *Biol. Reprod.* **32**, 979-987.

Hirshfield, A. N. (1989). Granulosa cell proliferation in very small follicles of cycling rats studied by long-term continuous tritiated-thymidine infusion. *Biol. Reprod.* **41**, 309-316.

Hirshfield, A. N. (1991). Development of follicles in the mammalian ovary. *Int. Rev. Cytol.* **124**, 43-101.

Hosoyamada, Y. and Sakai, T. (2003). The ultrastructure of periductal connective tissue and distinctive populations of collagen fibrils associated with ductal epithelia of exocrine glands. *Arch. Histol. Cytol.* **66**, 407-418.

Huet, C., Pisselet, C., Mandon-Pepin, B., Monget, P. and Monniaux, D. (2001). Extracellular matrix regulates ovine granulosa cell survival, proliferation and steroidogenesis: relationships between cell shape and function. *J. Endocrinol.* **169**, 347-360.

Hussein, T. S., Froiland, D. A., Amato, F., Thompson, J. G. and Gilchrist, R. B. (2005). Oocytes prevent cumulus cell apoptosis by maintaining a morphogenic paracrine gradient of bone morphogenetic proteins. *J. Cell Sci.* **118**, 5257-5268.

Ingber, D. E. (2004). The mechanochemical basis of cell and tissue regulation. *Mech. Chem. Biosyst.* **1**, 53-68.

Kreeger, P. K., Fernandes, N. N., Woodruff, T. K. and Shea, L. D. (2005). Regulation of mouse follicle development by follicle-stimulating hormone in a three-dimensional in vitro culture system is dependent on follicle stage and dose. *Biol. Reprod.* **73**, 942-950.

Laskey, R. (2005). The Croonian Lecture 2001 hunting the antisocial cancer cell: MCM proteins and their exploitation. *Philos. Trans. R. Soc. Lond., B, Biol. Sci.* **360**, 1119-1132.

LeBleu, V. S., Macdonald, B. and Kalluri, R. (2007). Structure and function of basement membranes. *Exp. Biol. Med. (Maywood)* **232**, 1121-1129.

Lechler, T. and Fuchs, E. (2005). Asymmetric cell divisions promote stratification and differentiation of mammalian skin. *Nature* **437**, 275-280.

Lundy, T., Smith, P., O'Connell, A., Hudson, N. L. and McNatty, K. P. (1999). Populations of granulosa cells in small follicles of the sheep ovary. *J. Reprod. Fertil.* **115**, 251-262.

Matzuk, M. M. and Lamb, D. J. (2002). Genetic dissection of mammalian fertility pathways. *Nat. Cell Biol.* **4**, S41-S49.

Matzuk, M. M., Burns, K. H., Viveiros, M. M. and Eppig, J. J. (2002). Intercellular communication in the mammalian ovary: oocytes carry the conversation. *Science* **296**, 2178-2180.

Meredith, S., Dudenhoeffer, G. and Jackson, K. (2000). Classification of small type B/C follicles as primordial follicles in mature rats. *J. Reprod. Fertil.* **119**, 43-48.

Mizunuma, H., Liu, X., Andoh, K., Abe, Y., Kobayashi, J., Yamada, K., Yokota, H., Ibuki, Y. and Hasegawa, Y. (1999). Activin from secondary follicles causes small preantral follicles to remain dormant at the resting stage. *Endocrinology* **140**, 37-42.

Monniaux, D., Huet-Calderwood, C., Le Bellego, F., Fabre, S., Monget, P. and Calderwood, D. A. (2006). Integrins in the ovary. *Semin. Reprod. Med.* **24**, 251-261.

O'Connell, C. B. and Wang, Y. L. (2000). Mammalian spindle orientation and position respond to changes in cell shape in a dynein-dependent fashion. *Mol. Biol. Cell* **11**, 1765-1774.

O'Shaughnessy, P. J., Dudley, K. and Rajapaksha, W. R. (1996). Expression of follicle stimulating hormone-receptor mRNA during gonadal development. *Mol. Cell. Endocrinol.* **125**, 169-175.

O'Shaughnessy, P. J., McLelland, D. and McBride, M. W. (1997). Regulation of luteinizing hormone-receptor and follicle-stimulating hormone-receptor messenger ribonucleic acid levels during development in the neonatal mouse ovary. *Biol. Reprod.* **57**, 602-608.

Oktay, K., Schenken, R. S. and Nelson, J. F. (1995). Proliferating cell nuclear antigen marks the initiation of follicular growth in the rat. *Biol. Reprod.* **53**, 295-301.

Oktay, K., Karlikaya, G., Akman, O., Ojakian, G. K. and Oktay, M. (2000). Interaction of extracellular matrix and activin-A in the initiation of follicle growth in the mouse ovary. *Biol. Reprod.* **63**, 457-461.

Pedersen, T. (1969). Follicle growth in the immature mouse ovary. *Acta Endocrinol.* **62**, 117-132.

Picton, H. M. (2001). Activation of follicle development: the primordial follicle. *Theriogenology* **55**, 1193-1210.

Rodgers, R. J., Irving-Rodgers, H. F. and Russell, D. L. (2003). Extracellular matrix of the developing ovarian follicle. *Reproduction* **126**, 415-424.

Roy, S. K. and Greenwald, G. S. (1989). Hormonal requirements for the growth and differentiation of hamster preantral follicles in long-term culture. *J. Reprod. Fertil.* **87**, 103-114.

Stiff, M. E., Bronson, F. H. and Stetson, M. H. (1974). Plasma gonadotropins in prenatal and prepubertal female mice: disorganization of pubertal cycles in the absence of a male. *Endocrinology* **94**, 492-496.

Stubbs, S. A., Hardy, K., Da Silva-Buttkus, P., Stark, J., Webber, L. J., Flanagan, A. M., Themmen, A. P., Visser, J. A., Groome, N. P. and Franks, S. (2005). Anti-mullerian hormone protein expression is reduced during the initial stages of follicle development in human polycystic ovaries. *J. Clin. Endocrinol. Metab.* **90**, 5536-5543.

Stubbs, S. A., Stark, J., Dilworth, S. M., Franks, S. and Hardy, K. (2007). Abnormal preantral folliculogenesis in polycystic ovaries is associated with increased granulosa cell division. *J. Clin. Endocrinol. Metab.* **92**, 4418-4426.

Thery, M. and Bornens, M. (2006). Cell shape and cell division. *Curr. Opin. Cell Biol.* **18**, 648-657.

Uda, M., Ottolenghi, C., Crisponi, L., Garcia, J. E., Deiana, M., Kimber, W., Forabosco, A., Cao, A., Schlessinger, D. and Pilia, G. (2004). Foxl2 disruption causes mouse ovarian failure by pervasive blockage of follicle development. *Hum. Mol. Genet.* **13**, 1171-1181.

van Wezel, I. L., Krupa, M. and Rodgers, R. J. (1999). Development of the membrana granulosa of bovine antral follicles: structure, location of mitosis and pyknosis, and immunolocalization of involucrin and vimentin. *Reprod. Fertil. Dev.* **11**, 37-48.

Wandji, S. A., Srsen, V., Voss, A. K., Eppig, J. J. and Fortune, J. E. (1996). Initiation *in vitro* of growth of bovine primordial follicles. *Biol. Reprod.* **55**, 942-948.

Wandji, S. A., Srsen, V., Nathanielsz, P. W., Eppig, J. J. and Fortune, J. E. (1997). Initiation of growth of baboon primordial follicles *in vitro*. *Hum. Reprod.* **12**, 1993-2001.

Xu, M., West, E., Shea, L. D. and Woodruff, T. K. (2006). Identification of a stage-specific permissive *in vitro* culture environment for follicle growth and oocyte development. *Biol. Reprod.* **75**, 916-923.

Zamboni, L. (1974). Fine morphology of the follicle wall and follicle cell-oocyte association. *Biol. Reprod.* **10**, 125-149.